

Screening properties of the two-dimensional electron gas in the quantum Hall regime

Ulrich Wulf, Vidar Gudmundsson, and Rolf R. Gerhardt

Max-Planck-Institut für Festkörperforschung, Heisenbergstrasse 1, D-7000 Stuttgart 80, Federal Republic of Germany

(Received 9 November 1987; revised manuscript received 4 April 1988)

The screening properties of a two-dimensional electron gas (2D EG) in a quantizing magnetic field at low temperatures are calculated within the Hartree approximation. The effect of a periodic external potential on the equilibrium state is studied for two models of the 2D EG, a strictly two-dimensional Hall strip geometry and a three-dimensional model of a heterostructure without lateral confinement. The single-particle energy spectrum is found to depend drastically on the collective state of the 2D EG, i.e., the position of the Fermi energy with respect to the Landau levels. Strong nonlinear effects, such as perfect screening in only a part of the sample and pinning of the energy spectrum to the Fermi level, are observed.

I. INTRODUCTION

In this paper we investigate the screening properties of a two-dimensional electron gas (2D EG) in a strong perpendicular magnetic field \mathbf{B} .¹ This is an interesting problem on its own right, since due to the Landau quantization the screening is highly nonlinear and strongly B dependent. From qualitative arguments surprising effects such as perfect screening in certain subregions and partial pinning of the single-particle energy spectrum to the Fermi level have been predicted² for the 2D EG in a fluctuating external potential which varies slowly on the scale of the magnetic length $l = (eB/\hbar c)^{-1/2}$. Such effects are important for an understanding of the spatial distribution of charge and current density in the quantum Hall effect (QHE).

On the other hand, these intriguing screening properties play an important—though not obvious—role for the understanding of recent measurements of the capacitance,^{3–6} the activation energy,^{3,6–9} the gate voltage and current,^{3,6,10,11} the specific heat,¹² and the magnetization,¹³ which yield information about the thermodynamic density of states at the Fermi level, i.e., the derivative of the electron density n_s with respect to the chemical potential μ , $D_T = \partial n_s / \partial \mu$. For both, Si metal-oxide-semiconductor field-effect transistors (MOSFET's) and GaAs/Al_xGa_{1-x}As heterostructures, unexpectedly large values of D_T everywhere between adjacent Landau levels (LL's) have been obtained even in strong magnetic fields, where the LL's are well separated. Early attempts to explain these experiments neglected many-body effects and assumed a single-particle density of states (DOS) with a constant background underlying Gaussian shaped broadened LL's. Recently it became clear, however, that the experimental findings can be understood as a consequence of an oscillatory dependence of the effective linewidth on the filling factor $\nu = 2\pi l^2 n_s$ of the LL's, i.e., a many-body effect related to the screening of long-range charge-density fluctuations by the 2D EG.

Clear experimental evidence for oscillations of the linewidth of LL's as a function of ν has recently been ob-

tained from cyclotron resonance measurements¹⁴ and, more directly, from the beautiful luminescence measurements by Kukushkin and Timofeev,^{15,16} which yield an immediate image of the density of states in the whole conduction-band region below the Fermi level. As they demonstrate, the width of the LL's oscillates as a function of the filling factor ν showing pronounced maxima for complete filling of the levels. Correspondingly, the value of the DOS in the middle between two adjacent LL's is an oscillatory function of the position of the Fermi level μ , being maximum if μ is well between adjacent Landau levels and being essentially zero if μ is in the middle of a broadened level.¹⁶

The physical origin of these oscillations is screening of long-range charge-density fluctuations by the 2D EG. Several authors^{17–20} have calculated an oscillating linewidth owing to the scattering of electrons by randomly distributed charged impurities. Screening of the impurity potentials was treated in the conventional linear approximation in terms of a dielectric function which reflects the oscillatory behavior of the DOS. The simplest reasonable approximations were used to calculate the linewidth from the screened impurity potentials. Since the linewidth in turn determines the dielectric function, we refer to these calculations as self-consistent screening theories (SCST's). They emphasize the origin of the oscillations: the DOS at the Fermi level. If this is large (μ within a LL), the electrons effectively screen the scattering potentials and the linewidth becomes small. If the DOS is small (μ between adjacent LL's), screening is poor and strong scattering potentials lead to a large linewidth and eventually to broad overlapping Landau levels.

Apart from the general trends, the predictions of the SCST's are, however, not reliable, especially in the poor screening situation. The scattering effects of the individual long-range impurity potentials are added incoherently in these theories which leads to very large values for the linewidth. In reality, the electrons interact with the coherent superposition of impurity potentials so that the linewidth is affected by the long-range tails of the

impurity potentials only via long-range *fluctuations of the impurity density*, not by the impurity density itself.

In a recent series of papers^{21–23} a “statistical inhomogeneity model” has been investigated which distinguishes between two different length scales on which a random array of charged impurities (such as donors in the barrier of a $\text{Al}_x\text{Ga}_{1-x}\text{As}$ heterostructure) affects the 2D EG differently. Short-range potential fluctuations on the scale of typical interelectronic distances ($\approx 100 \text{ \AA}$) are assumed to lead to a level broadening, as usual. A Gaussian line shape of the broadened LL’s is assumed.²⁴ Fluctuations of the impurity density on a mesoscopic length scale of 10^4 \AA , which lead to an inhomogeneous density distribution of the screening 2D EG, are taken into account by an ensemble average over homogeneous systems with a statistical distribution of electron densities n_s . The experimental results^{1,3–11} on the apparent background DOS are nicely reproduced by the statistical inhomogeneity model with a density fluctuation of the order of 1%.^{11,23} Fluctuations of this order of magnitude and a corresponding effect on the apparent inter-LL DOS must be expected,²⁵ since for a typical value of $n_s \lesssim 10^{12} \text{ cm}^{-2}$ an area of the order $(10^4 \text{ \AA})^2$ contains an average number of $N \lesssim 10^4$ electrons with a statistical fluctuation $\Delta N/N \sim N^{-1/2} \gtrsim 10^{-2}$. In the statistical inhomogeneity model the magnetic field dependence of the density fluctuation Δn_s was treated as a phenomenological input. In the spirit of the model one should, however, calculate this dependence from the magnetic-field-dependent screening of an inhomogeneous external electrostatic potential by the 2D EG. A major aim of our paper is to present such calculations and thus to complete our understanding of the “DOS measurements”.^{3–13,15,16}

In the present paper we neglect short-range potential fluctuations such as arising from individual, randomly distributed charged impurities completely. We concentrate, instead, on the screening of a given external electrostatic potential $V(\mathbf{r})$, which varies slowly on the scale of the magnetic length, thus satisfying $l | \nabla V | \ll \hbar \omega_c$ with $\omega_c = eB/mc$ the cyclotron frequency. We will, however, allow the total variation of $V(\mathbf{r})$ over long distances to be large, $\max | V(\mathbf{r}) - \bar{V} | \gtrsim \hbar \omega_c$, where \bar{V} is the spatial average of $V(\mathbf{r})$. As a simple but typical example we will consider external potentials which modulate the 2D EG only in one direction. This keeps the mathematical treatment simple and is also of relevance to recent experiments on the modulated 2D EG in heterostructures with a microstructured linear-grating gate.²⁶

We emphasize that, for the problems of our present interest, we cannot use the methods which have been developed in the SCST’s. These theories are most adequate for the case of randomly distributed, effectively screened, and thus short-range, Coulomb scatterers. Averaging over the impurity configurations is an important ingredient of these theories and leads to a spatially homogeneous situation with an averaged Green’s function depending only on the Landau quantum number but not on the center-coordinate quantum number x_0 (cf. Sec. III below), and to imaginary parts of self-energy and Green’s function which determine the level broadening. The scattering potentials are screened with a dielectric

function which self-consistently contains level broadening effects due to the screened scattering potentials. This is a type of self-consistent-field approximation for the scattering potentials, of the same kind as the calculation of self-energy contributions with the dressed Green’s function. This mean-field approximation for the scattering potentials is adequate for the averaged system and is made in addition to the random-phase approximation for the mutual Coulomb interaction between the electrons.

The situation of our present interest is, however, very different. We consider a fixed spatially varying external potential and ask for the corresponding equilibrium values of the position-dependent electron density and the screened potential. There is no averaging over impurity configurations, and no imaginary parts are introduced. The varying potential lifts, however, the degeneracy of the Landau levels, and the energy eigenvalues become dependent on the center coordinate x_0 , with the periodicity of the external potential, so that one may speak of a “broadening” of the Landau levels into bands of finite width. We solve the problem within the Hartree approximation, i.e., we treat the mutual Coulomb interaction between electrons in a self-consistent-field approximation where the electrostatic potential for a given electron density distribution is derived from Poisson’s equation. The electron density for a given effective potential is, in turn, evaluated from the exact Schrödinger equation, without using any perturbation expansion or linear-response assumptions as in the SCST’s. A further difference concerns the mixing of Landau levels. In the SCST’s large level widths are calculated^{18–20} for completely filled Landau levels which lead to a considerable overlap of adjacent levels, and thus the mixing of Landau levels by the scattering potentials should be taken into account. Here we consider, on the other hand, only slowly varying potentials $V(x)$ with $l | dV/dx | < \hbar \omega_c$. Thus, the local mixing of Landau levels at a given center coordinate x_0 by $V(x)$ is not very important. Nevertheless, we take it into account in the numerical calculations by diagonalizing a sufficiently large matrix. We will show, however, that long-range electrostatic forces prohibit an overlap of the Landau bands, $E_{n+1}(x_0) \geq E_n(x'_0)$ for all x_0 and x'_0 . This type of level repulsion also cannot be treated by the methods of the SCST’s. For these reasons, we use the mentioned Hartree approximation for our numerical calculations.

Recently an analytical consideration of screening effects based on the same Hartree approximation has been given by Labbé.²⁷ He derives a set of nonlinear equations for the Fourier coefficients of the screened potential, but does not attempt to solve it explicitly. Labbé does not mention any of the peculiar nonlinear screening effects which are calculated and discussed in the present paper.

In Sec. II we demonstrate that the conventional linear theory of screening is applicable only if a Landau level is nearly half-filled. Then the screening is perfect in the low-temperature limit. If the LL is nearly full or nearly empty, the linear approximation breaks down. We, therefore, calculate without linearization the response of the 2D EG to an external modulating potential self-

consistently in the Hartree approximation. This yields the energy spectrum of the electron states, the modulated electron density, and the total (screened) potential. The calculations are performed for two models which are described in Sec. III. In one of the models the 2D EG is confined to a strip geometry, so that boundary effects can be studied. The results are presented and discussed in Sec. IV. A brief summary is given in Sec. V.

II. LINEAR SCREENING APPROXIMATION

A. Thomas-Fermi theory

For a better understanding of the screening properties of the 2D EG it is instructive to consider the conventional Thomas-Fermi approach.

The three-dimensional solution

$$\phi(\mathbf{r}) = \int d^3r' \frac{\rho(x', y', \delta(z'))}{\kappa |\mathbf{r} - \mathbf{r}'|} \quad (2.1)$$

of Poisson's equation in a medium with a dielectric constant κ ($\kappa = 12.4$ in GaAs), determines the potential energy $V(x, y) = -e\phi(x, y, 0)$ of the 2D electrons,

$$V(\mathbf{R}) = -\frac{e}{\kappa} \int d^2R' \frac{1}{|\mathbf{R} - \mathbf{R}'|} \rho(\mathbf{R}') . \quad (2.2)$$

Taking 2D Fourier transforms, we have

$$V(\mathbf{K}) = -\frac{2\pi e}{\kappa |\mathbf{K}|} \rho(\mathbf{K}) . \quad (2.3)$$

The charge density is written as

$$\rho(\mathbf{R}) = e[\bar{n} + \delta n_{\text{ext}}(\mathbf{R})] - en_s(\mathbf{R}) , \quad (2.4)$$

where \bar{n} compensates the average electron charge density, and the perturbation $e\delta n_{\text{ext}}$ is the source of an external potential

$$V_{\text{ext}}(\mathbf{K}) = -\frac{2\pi e^2}{\kappa K} \delta n_{\text{ext}}(\mathbf{K}) . \quad (2.5)$$

For an $\text{Al}_x\text{Ga}_{1-x}\text{As}$ heterostructure with $2\pi/K \sim 10^{-4}$ cm and $\delta n_{\text{ext}}(\mathbf{K}) \sim 10^{10}$ cm $^{-2}$ one obtains $|V_{\text{ext}}(\mathbf{K})| \sim 10$ meV. For a system with a microstructured gate near the one-dimensional transition,²⁶ $2\pi/K \sim 500$ nm and $\delta n_{\text{ext}} \sim 10^{11}$ cm $^{-2}$, $|V_{\text{ext}}(\mathbf{K})| \sim 60$ meV.

Of course, we can also consider an external potential in Eq. (2.3) which is generated by external charges outside the plane of the 2D EG. As usual within the Thomas-Fermi approximation, we assume that the total potential varies slowly on the microscopic scale, so that it can be treated similar to a thermodynamic variable in an inhomogeneous system. In the case of our present interest that means slow variation on the scale of the magnetic length, $l |\nabla V| \ll \hbar\omega_c$. Then the electron density is given by

$$n_s(\mathbf{R}) = \int dE D(E) f[E + V(\mathbf{R}) - \mu] , \quad (2.6)$$

with $D(E)$ the density of states of the 2D EG and $f(E) = [\exp(E/k_B T) + 1]^{-1}$ the Fermi function at temperature T . Linearizing with respect to V ,

$$n_s(\mathbf{R}) = \bar{n}_s - D_T V(\mathbf{R}) , \quad (2.7)$$

where

$$D_T = \frac{\partial \bar{n}_s}{\partial \mu} = - \int dE D(E) \frac{d}{dE} f(E - \mu) \quad (2.8)$$

is the thermodynamic density of states, we obtain the linear screening approximation

$$V(\mathbf{K}) = V_{\text{ext}}(\mathbf{K}) - \frac{2\pi e^2}{\kappa K} D_T V(\mathbf{K}) . \quad (2.9)$$

Thus we find $V(\mathbf{K}) = V_{\text{ext}}(\mathbf{K})/\epsilon(\mathbf{K})$ with the dielectric function

$$\epsilon(\mathbf{K}) = 1 + \frac{Q}{|\mathbf{K}|} , \quad (2.10)$$

where the Thomas-Fermi wave vector

$$Q = 2\pi \frac{e^2}{\kappa} D_T \quad (2.11)$$

defines the screening length $2\pi/Q$.

B. "Perfect" screening

With the bare Landau density of states

$$D(E) = \frac{2}{2\pi l^2} \sum_{n=0}^{\infty} \delta(E - \hbar\omega_c(n + \frac{1}{2})) , \quad (2.12)$$

we obtain for $k_B T \ll \hbar\omega_c$ (well separated LL's),

$$2\pi l^2 \bar{n}_s \equiv \bar{\nu} = 2n + \bar{\nu}_n , \quad (2.13)$$

where $n \geq 0$ is the number of the partially filled LL and $\bar{\nu}_n$ (with $0 < \bar{\nu}_n \leq 2$) its filling factor in the homogeneous 2D EG. Inserting Eq. (2.12) into (2.8), we find

$$D_T = \frac{1}{k_B T} \frac{\bar{\nu}_n}{2} \left[1 - \frac{\bar{\nu}_n}{2} \right] \frac{2}{2\pi l^2} \quad (2.14)$$

and

$$Q = \frac{\hbar\omega_c}{k_B T} \frac{\bar{\nu}_n}{2} \left[1 - \frac{\bar{\nu}_n}{2} \right] Q_0 , \quad (2.15)$$

where

$$Q_0 = \frac{2\pi e^2}{\kappa} \left[\frac{m}{\pi \hbar^2} \right] = \frac{2}{a_B} \quad (2.16)$$

is the Thomas-Fermi wave vector for zero magnetic field, which is simply given by the effective Bohr radius a_B . For strong magnetic field and low temperature, the values of Q and $\epsilon(\mathbf{K})$ may become very large meaning the screening becomes much more effective than for zero magnetic field. This result agrees to leading order in the small quantity $l |\mathbf{K}|$ with Labbé's dielectric constant,²⁷ if we replace $\bar{\nu}_n/2$ with $\bar{\nu}_n$, i.e., neglect the spin degeneracy.

In the numerical calculations we consider a sinusoidal modulation of the positively charged background with a period of the order of $a \approx 18a_B$. For $B = 0$, the electrons will partly screen the external potential caused by this

modulation so that the effective potential oscillates with an amplitude which is about a factor of 7 smaller than the amplitude of the external potential. In a magnetic field of about $6T$ ($\hbar\omega_c \approx 10$ meV for GaAs) and at a temperature of 1 K ($k_B T \approx 0.1$ meV), on the other hand, the screening can be much better, with the amplitude of the total potential about two orders of magnitude smaller than that of the external potential, provided the average filling factor $\bar{\nu}$ is close to an odd integer.

C. Breakdown of linear screening

For zero magnetic field the density of states is constant, $D_0 = m / \pi \hbar^2$. Then for $k_B T \ll \mu$ the mean electron density \bar{n}_s increases linearly with increasing μ , and the linear approximation of Eq. (2.7) is essentially exact.

In a strong magnetic field, however, $\bar{n}_s(\mu)$ is a broadened step function and the linear approximation is only valid if $\max(|V(\mathbf{R}) - \bar{V}|) < \beta k_B T$, with $1 \lesssim \beta \lesssim 2$. For a sinusoidal modulation of the background density, $\delta n_{\text{ext}}(\mathbf{R}) = \gamma \bar{n} \cos(2\pi x/a)$, the total screened potential in the linear screening regime is

$$V(\mathbf{R}) = -V_0 \cos(2\pi x/a), \quad V_0 = \frac{\gamma \bar{n} e^2 a}{\kappa(1 + Qa/2\pi)}, \quad (2.17)$$

and the condition for linear screening becomes

$$\gamma \bar{n} e^2 a / \kappa < \beta \left[k_B T + \hbar\omega_c \frac{\bar{\nu}_n}{2} \left(1 - \frac{\bar{\nu}_n}{2} \right) \frac{a}{\pi a_B} \right]. \quad (2.18)$$

In the low-temperature limit, $k_B T \ll \hbar\omega_c$, the amplitude of the screened potential becomes proportional to $k_B T$, and condition (2.18) reduces to

$$\frac{\gamma \bar{\nu}}{2} \equiv \frac{\gamma(2n + \bar{\nu}_n)}{2} < \beta \frac{\bar{\nu}_n}{2} \left(1 - \frac{\bar{\nu}_n}{2} \right). \quad (2.19)$$

This is satisfied if the density modulation is not too large ($\gamma \lesssim 0.5$), the magnetic field is not too small (n small), and if the average filling factor $\bar{\nu}_n$ is not too close to 0 or 2. Note that (2.19) is independent of the period a of the density modulation. Nevertheless, perfect screening can no longer be expected if a becomes too small, i.e., of the order of the magnetic length or less, since then Eq. (2.6) breaks down.

Let us assume a situation with perfect screening and with μ in the lowest LL ($n=0$). If now the magnetic field is lowered, the filling factor $\bar{\nu}_0$ increases towards 2, the amplitude V_0 of the total potential, Eq. (2.17), increases, and the condition (2.18) for perfect screening breaks down. Since $k_B T \ll \hbar\omega_c$ still holds, the electron density $n_s(\mathbf{R})$ near the minima of $V(\mathbf{R})$, i.e., near the maxima of $\delta n_{\text{ext}}(\mathbf{R})$, is cut off at a value $2/(2\pi l^2)$, whereas near the minima of δn_{ext} the electron density $n_s(\mathbf{R})$ can still follow the external modulation. As a consequence, the 2D EG responds with an anharmonic density distribution on a harmonic external perturbation. In this regime the screening becomes strongly nonlinear and perfect screening can pertain in certain space regions whereas screening breaks down in others. In order to de-

scribe this situation adequately, we have to go beyond the linear screening approximation.

III. THE HARTREE APPROACH

A. Self-consistent equations

We consider the ground state of a 2D EG in the x - y plane with a perpendicular magnetic field. The electrostatic potential is assumed to be homogeneous only in the y direction thus allowing for a modulation of the electron density in the x direction. The single-particle Hamiltonian in the mean-field approximation is

$$H = \sum_i \frac{\left[p_i + \frac{e}{c} A_i \right]^2}{2m_i} + V, \quad (3.1)$$

where V is the effective electrostatic potential, \mathbf{A} the vector potential due to the magnetic field, and m_i are the effective masses (setting $m_x = m_y = m$). V is determined by the external charges and by the mutual interaction of the electrons. The latter is described in the Hartree approximation, so that it satisfies Poisson's equation,

$$\Delta V = \frac{4\pi e}{\kappa} (-en_s + \rho_b), \quad (3.2)$$

where n_s and ρ_b are the volume densities of the electrons and the background charges. In the Landau gauge $\mathbf{A} = (0, Bx, 0)$ and with periodic boundary conditions in the y direction the normalized eigenfunctions can be written as

$$\Psi_\lambda(x, y, z) = \Phi_\lambda(x, z) \exp(ik_y y), \quad (3.3)$$

leading to the reduced Hamiltonian

$$H = -\frac{\hbar^2}{2m} \frac{\partial^2}{\partial x^2} - \frac{\hbar^2}{2m_z} \frac{\partial^2}{\partial z^2} + \frac{1}{2} m \omega_c^2 (x - x_0)^2 + V, \quad (3.4)$$

with $x_0 = -l^2 k_y$. The density is obtained from the eigenfunctions and their occupation $f(E_\lambda - \mu)$ by

$$n_s(x, z) = g \sum_\lambda f(E_\lambda - \mu) |\Psi_\lambda(x, y, z)|^2, \quad (3.5)$$

where μ is the chemical potential, g a degeneracy factor, and E_λ the energy eigenvalue. Equations (3.2)–(3.5) will be solved self-consistently for two models of the 2D EG and the external charges.

B. Three-dimensional model

In this model one proceeds from a metal-insulator semiconductor (MIS) structure with a microstructured gate as in Ref. 28 (see Fig. 1) with a magnetic field imposed. The actual microstructure of the gate is represented by the boundary condition

$$V(x, z = -D_{\text{ins}}) = V_G + V_M \cos(k_0 x). \quad (3.6)$$

The parameters V_G and V_M determine the average elec-

tron density and the degree of its modulation respectively, $k_0 = 2\pi/a$ is the wave vector of the gate structure with the period a . The system is strictly periodical in the x direction and therefore a Fourier expansion

$$-en_s(x,z) + \rho_b(x,z) = -e \sum_r [n_{s,r}(z) + n_{d,r}(z)] \exp(-iq_r x), \quad (3.7)$$

$$V(x,z) = \sum_r V_r(z) \exp(-iq_r x),$$

$$q_r = rk_0, \quad r = 0, \pm 1, \pm 2, \dots \quad (3.8)$$

is performed. Here the background charge ρ_b has been identified with the charge $-en_d$ of the depletion layer. The solution of Eq. (3.2) is then found to be

$$V_{r \neq 0}(z > 0) = \frac{\epsilon V_M}{\epsilon \cosh(|q_r| D_{\text{ins}}) + \sinh(|q_r| D_{\text{ins}})} \frac{1}{2} \delta_{|q_r|, k_0} \exp(-|q_r| z) + \frac{2\pi e^2}{\kappa_{\text{sc}}} \int_0^\infty n_{s,r}(z') G_r(z', z) dz' + \frac{2\pi e^2}{\kappa_{\text{sc}}} \frac{\sinh(|q_r| D_{\text{ins}}) - \epsilon \cosh(|q_r| D_{\text{ins}})}{\sinh(|q_r| D_{\text{ins}}) + \epsilon \cosh(|q_r| D_{\text{ins}})} I_r \exp(-|q_r| z), \quad (3.9)$$

with

$$G_{r \neq 0}(z', z) = \frac{\exp(-|q_r| |z' - z|)}{|q_r|}, \quad (3.10a)$$

$$I_r = \frac{1}{|q_r|} \int_0^\infty \exp(-|q_r| z') n_{s,r}(z') dz', \quad (3.10b)$$

and

$$V_{r=0}(z > 0) = \frac{4\pi e^2}{\kappa_{\text{sc}}} \left[\left[N_{\text{depl}} + \frac{N_s}{2} \right] z - \frac{1}{2} \int_0^\infty n_{s,r=0}(z') (|z - z'| - z') dz' \right]. \quad (3.11)$$

We do not allow the electrons to penetrate into the insulator, $n_s(z) = 0$ for $z < 0$. κ_{ins} and κ_{sc} are the dielectric constants of the insulator and the semiconductor with $\epsilon = \kappa_{\text{ins}}/\kappa_{\text{sc}}$. N_{depl} and N_s represent the depletion and electron density per unit area averaged over one period of the microstructure potential. The first term of Eq. (3.9) is due to the external potential, the second to the Coulomb interaction, and the third to the image charges.

It is seen from the Hamiltonian in Eq. (3.4), that the behavior of the electrons in the x direction is dominated by $\frac{1}{2} m \omega_c^2 (x - x_0)^2$ for large values of $|x|$. Therefore the wave functions vanish in this limit according to their asymptotic form given by the Hermite functions. They also vanish for $z \leq 0$ and $z \rightarrow \infty$. The wave functions can therefore be expressed as

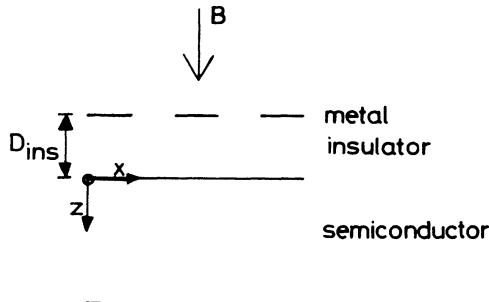


FIG. 1. Schematic geometry of the microstructured MIS system with an imposed normal magnetic field.

$$\Phi_\lambda(x,z) = \Phi_{M,N}^{x_0}(x,z), \quad (3.12)$$

where M and N denote the number of nodes in the x and z directions, respectively. The density is determined by

$$n_s(x,z) = g \sum_{x_0, M, N} f(E_{x_0, M, N} - \mu) |\Phi_{M,N}^{x_0}(x,z)|^2, \quad (3.13)$$

where x_0 is given by $k_y = n(2\pi/L_y)$, $n = 0, \pm 1, \pm 2, \dots$ and g is a degeneracy factor. The Fourier component of the density can be expressed as

$$n_{s,r}(z) = \lim_{L_x \rightarrow \infty} \frac{1}{L_x} \int_{-L_x/2}^{L_x/2} n_s(x,z) \exp(iq_r x) dx = g \sum_{x_0, M, N} f(E_{x_0, M, N} - \mu) \phi_r^{M, N, x_0}(z), \quad (3.14)$$

with

$$\phi_r^{M, N, x_0}(z) = \frac{1}{a} \int_{-\infty}^{\infty} |\Phi_{M,N}^{x_0}|^2 \exp(iq_r x) dx, \quad (3.15)$$

where we have exploited that $E_{x_0, M, N}$ and ϕ_r^{M, N, x_0} are invariant under translations $x_0 \rightarrow x_0 + a$. The tilde over the summation sign means that the x_0 summation has to be limited to a single period.

The Eqs. (3.4)–(3.15) establish the complete self-consistency problem, that is solved iteratively.

C. Two-dimensional model with edges

In this section we consider a strictly two-dimensional model, in which the electrons are confined to a Hall strip geometry. Within this model we are able to study the interplay between edge and “bulk” effects in the 2D system. The Schrödinger equation (3.4) reduces now to

$$\left[-\frac{\hbar^2}{2m} \frac{\partial^2}{\partial x^2} + \frac{1}{2} m \omega_c^2 (x - x_0)^2 + V(x) \right] \Phi(x) = E \Phi(x), \quad (3.16)$$

and the confinement in the x direction is obtained from the boundary conditions

$$\Phi(-L_x/2) = \Phi(L_x/2) = 0, \quad (3.17)$$

which describe the effect of infinitely high potential barriers at $x = \pm \frac{1}{2} L_x$. The Hartree potential $V(x)$ is given by Eq. (2.2), i.e., the electrostatic potential energy in the plane $z = 0$ of the 2D EG. The 2D charge density is assumed to be homogeneous in the y direction and written as

$$\rho(\mathbf{R}) = -en_s(x) + en_b(x), \quad (3.18)$$

where $n_b(x)$ is the density of a neutralizing background of positive charge. Then the y' integral in Eq. (2.2) can be performed analytically, leading to

$$V(x) = -\frac{2e^2}{\kappa} \int_{-L_x/2}^{L_x/2} dx' [n_s(x') - n_b(x')] \ln \left| \frac{x - x'}{L_x/2} \right|, \quad (3.19)$$

where charge neutrality has been assumed:

$$\int_{-L_x/2}^{L_x/2} dx' [n_s(x') - n_b(x')] = 0. \quad (3.20)$$

The electron density is given by

$$n_s(x) = \frac{g}{L_x L_y} \sum_{n, x_0} f(E_{n, x_0} - \mu) |\Phi_{n, x_0}(x)|^2, \quad (3.21)$$

where $\Phi_{n, x_0}(x)$ is the normalized eigenfunction of Eq. (3.16) with n nodes ($n = 0, 1, \dots$) and E_{n, x_0} the energy eigenvalue. We write

$$E_{n, x_0} = \hbar \omega_c \left[\nu_n(x_0) + \frac{1}{2} \right], \quad (3.22)$$

so that the real function $\nu_n(x_0)$ reduces to the Landau quantum number n , if the “center coordinate” x_0 is far away from the edges, $|L_x/2 - x_0| \gg l$ and $|-L_x/2 - x_0| \gg l$. The chemical potential μ is determined by the mean electron density

$$n_s = \frac{1}{L_x} \int_{-L_x/2}^{L_x/2} dx n_s(x) = \frac{g}{L_x L_y} \sum_{n, x_0} f(E_{n, x_0} - \mu). \quad (3.23)$$

For a given background density $n_b(x)$, Eqs. (3.16)–(3.22) must be solved self-consistently. We do this by a suitable iteration procedure. For practical reasons we expand the eigenfunctions in terms of the eigenfunctions of the un-

perturbed system, defined by Eqs. (3.16) and (3.17) with $V(x) \equiv 0$, which are linear combinations of parabolic-cylinder functions.²⁹ Within a suitable subspace of basis functions the Hamiltonian matrix is diagonalized in each iteration loop. The most convenient method to study screening properties within this model is to calculate the response of the system to modulations of the neutralizing rigid positive background.

IV. RESULTS AND DISCUSSION

In this section we present the results of the numerical calculations. We start with the three-dimensional model of Sec. III A which considers no boundaries in the plane of the 2D EG. Within this model we can study the response of the 2D EG to a strictly harmonic external potential, so that a close comparison of the numerical results with the predictions of the linear screening approximation of Sec. II is possible.

In Sec. IV B we consider the 2D EG with boundaries. For real Hall samples, the presence of boundaries is very important since it allows for the building up of the Hall field as a response to the current imposed on the sample. Near the boundaries the effective potential will vary rapidly so that the linear screening approximation cannot be expected to hold. So it is interesting to investigate the screening properties of the 2D EG near the edges and the effect of the edges on the screening properties of the bulk.

A. The three-dimensional model

For numerical calculations a GaAs-AlGaAs heterostructure is assumed ($\kappa_{sc} = 12.4$, $\kappa_{ins} = 11.6$, $m_z = m = 0.067m_0$, and $g = 2$). The insulator thickness and the period of the harmonic lateral modulation are chosen as $D_{ins} = 26$ nm and $2\pi/k_0 = 180$ nm, respectively. The average electron density is $n_s = 2.25 \times 10^{11}$ cm⁻², the density of the depletion charges $N_{depl} = 3 \times 10^{11}$ cm⁻². It follows from Eq. (3.11) that the external potential has a strong $r = 0$ component. Therefore, the behavior of the system in the z direction is approximately independent of the amplitude V_M of the modulating potential in all situations considered here. In the numerical calculations only the lowest electrical subband (a single Airy function) is taken into account. Furthermore, we consider sufficiently high values of the magnetic field, so that only the lowest two Landau levels ($n = 0, 1$) are partly occupied (we choose $\nu < 2.5$). The numerical calculations showed that it is sufficient to consider only three LL's for a correct description of screening effects in the first two LL's within this restriction. This was checked by taking into account up to eight LL's and is a consequence of the fact that, for a given x_0 value, the mixing of LL's is not very important, since the modulation potentials vary sufficiently slowly on the scale l . First, a weak density modulation ($V_M = 25$ meV, see Fig. 2) of the electron gas is studied at a temperature $T = 1$ K for several values of the magnetic field. Figure 3 shows the dependence of the energy eigenvalues on the center coordinate x_0 (cf. Sec. III). The external modulating potential causes the degeneracy of the Landau levels to be lifted, and Landau bands

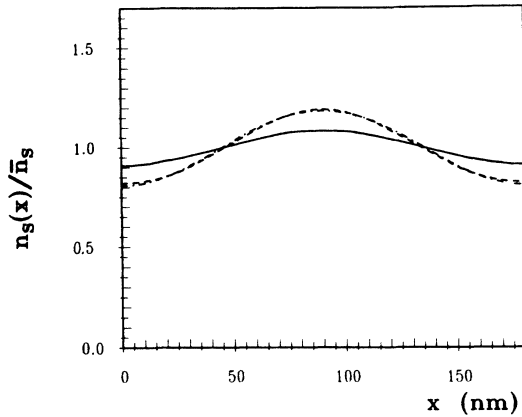


FIG. 2. Normalized electron density at $T=1$ K for three values of the filling factor: $\nu=2.4$ (dashed line), 2.0 (solid line), and 1.6 (dash-dotted line). The modulation in the x direction is due to a harmonic external potential of the amplitude $V_M=25$ meV at $z=-D_{\text{ins}}$. The electron density is shown at the z value where it is maximum.

of finite width develop. The energy zero is chosen such that the LL's of the homogeneous system appear at $\epsilon_B=(n+\frac{1}{2})\hbar\omega_c$. As seen from Fig. 3, for filling factors $\nu=1.6$ and $\nu=2.4$ the width of the Landau bands is very small, not much larger than $k_B T=0.1$ meV. This means that the external harmonic potential (see Fig. 4) is screened very effectively, as one expects from the linear screening theory of Sec. II. In agreement with the estimate Eq. (2.17), the screening for $\nu=1.6$ is better than for $\nu=2.4$, where the bandwidth is larger and the occurrence of higher harmonics in the screened potential (cf., Fig. 4) indicates the breakdown of linear screening.

As the filling factor approaches the value $\nu=2$, the screening properties change drastically. The linear screening approximation predicts at this filling factor no screening at all. The numerical results show, however, even for $\nu=2$ a considerable screening, so that the amplitude of the screened potential is substantially smaller than that of the external potential. The effect of the remaining screened potential on the energy spectrum is clearly seen in Fig. 3. The Landau bands show the same type of oscillation as the potential and the top of the "fully occupied" $n=0$ Landau band as well as the bottom of the "empty" $n=1$ Landau band appear at the Fermi energy. This result is, of course, not accidental. It is just the situation in which the thermal redistribution of electrons between the $n=0$ and the $n=1$ bands produces a screened potential with a total variation $\hbar\omega_c$ (within an accuracy of about $k_B T$). The screening cannot be weaker, since then the total (screened) potential would vary by more than $\hbar\omega_c$. This, however, would imply an overlap of the $n=0$ and the $n=1$ bands at the Fermi energy and, consequently, partially filled bands and high screening ability. Therefore, the self-consistent situation at $\nu=2$ is one in which both bands just touch the Fermi level. Since this is an important result, we explain it again in a slightly different way. If the total variation of the external potential is less than $\hbar\omega_c$, we expect for filling factor

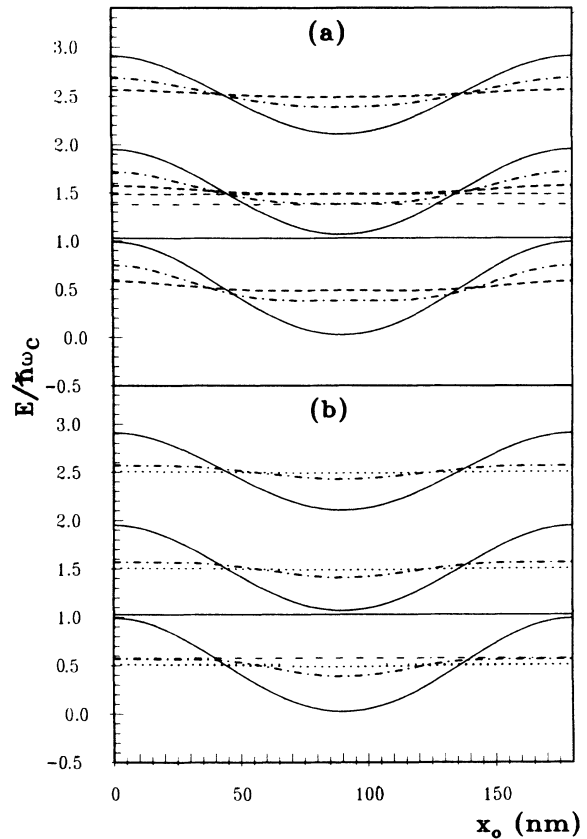


FIG. 3. Landau bands (thick lines) and corresponding Fermi levels (thin horizontal lines) for $V_M=25$ meV, $T=1$ K, and different values of the filling factor: (a) $\nu=2.0$ (solid lines), 2.3 (dash-dotted lines), 2.4 (broken lines); (b) $\nu=2.0$ (solid lines), 1.7 (dash-dotted lines), and 1.6 (dotted lines).

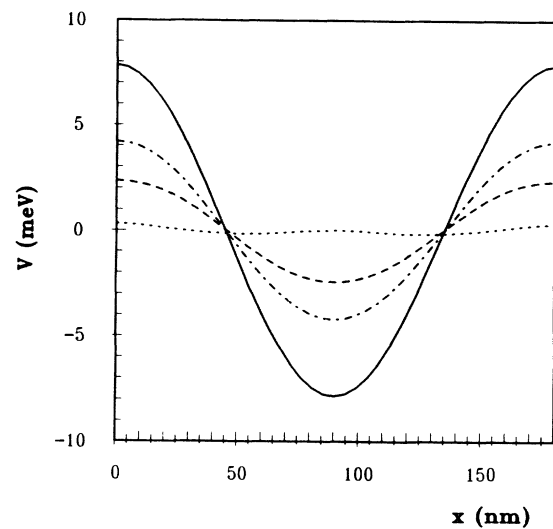


FIG. 4. External potential (solid line) for $V_M=25$ meV and the corresponding self-consistently screened potential at $\nu=2.0$, $T=1$ K (dash-dotted line), $\nu=2.0$, $T=10$ K (dashed line), and $\nu=2.4$, $T=1$ K (dotted line), respectively. The z value is taken at the maximum of the electron density distribution as in Fig. 2.

$\nu=2$ essentially no screening. The lowest LL is completely occupied, the electron density is constant. If the total variation of the external potential is, however, somewhat larger than $\hbar\omega_c$, the situation is different. If we assume no screening for $\nu=2$, as the linear theory predicts, we get a pattern of alternating stripes of high electron density, where the $n=0$ and the $n=1$ states are occupied, and stripes of low density, where $E_{n=0,x_0} > E_F$ and no states are occupied. This density modulation induces an electrostatic potential which screens the external potential, contrary to our assumption. Thus we see that there must be some screening, which requires a redistribution of electrons between the $n=0$ and the $n=1$ Landau bands and is possible if both are close to the Fermi level but do not overlap too much. As a result, the total variation of the screened potential will be close to $\hbar\omega_c$. We want to emphasize that the relatively large screening for $\nu=2$ (i.e., $\hbar\omega_c \approx 8.4$ meV and $l = 12$ nm) is a consequence of the large total variation of the external potential, $\Delta V_{\text{ext}} \approx 16$ meV $> \hbar\omega_c$ (cf. Fig. 4), and not a consequence of a large local electric field. The maximum electric field is here of the order of 0.02 mV/Å, and $|dV_{\text{ext}}/dx| l/\hbar\omega_c \approx 0.25$. The same type of nonlinear screening is expected if the same ΔV_{ext} results from a modulation with a larger period and, therefore, a smaller electric field. We do not present such results, since in our approach the computation time increases rapidly with the modulation period a . On the other hand, much larger electric fields can be produced in microstructured heterostructures. Using Eq. (2.5) one estimates from the data given by Hansen *et al.*²⁶ that the 2D EG in their sample splits into one-dimensional channels if the total variation of the external potential exceeds $\Delta V_{\text{ext}} \sim 200$ meV. For a period $a = 500$ nm, this implies an electric field of the order of 0.1 mV/Å. Whether or not an external potential can be screened by the 2D EG depends, however, mainly on the total variation ΔV_{ext} , and not on the local electric field. A further demonstration of this fact will be given below.

If the filling factor is increased above the value 2 by lowering the magnetic field, the states in the $n=1$ Landau band with center coordinates x_0 near the potential minimum are occupied first. Thus, the electron density increases near the potential minimum, but decreases near its maxima, since the degeneracy factor of the $n=0$ LL becomes smaller. As a result, the screening of the potential becomes better and the Landau bands become smaller, while the bottom of the $n=1$ band is pinned to the Fermi level [see Fig. 3(a), $\nu=2.3$]. Finally the screening becomes nearly perfect [Fig. 3(a), $\nu=2.4$]. If the filling factor is lowered below the value 2, the states with x_0 near the potential maxima are depopulated first. Again the screening becomes better and the bands become smaller, but now the Fermi level is pinned to the top of the $n=0$ band [Fig. 3(b), $\nu=1.7$].

Starting from the nearly perfect screening situation [Fig. 3(b), $\nu=1.7$] we understand the same results as follows. If the filling factor approaches 2 from below, the states with center coordinates x_0 close to the minimum of the screened potential (the state with minimum energy)

are completely occupied first. If the magnetic field decreases (ν increases) further, the electron density near the potential minimum decreases and the screening in this region breaks down. As a consequence, a pronounced minimum of the total potential, and thus of the energy spectrum, develops, whereas perfect screening persists at the top of the $n=0$ Landau level, which remains pinned to the Fermi energy [Fig. 3(b), $\nu=1.7$].

Figure 5 shows the variance

$$\frac{\Delta n_s}{n_s} = \left[\frac{1}{L_x} \int_{-L_x/2}^{L_x/2} \frac{[n_s(x) - n_s]^2}{n_s^2} dx \right]^{1/2} \quad (4.1)$$

of the electron density $n_s(x)$. In situations with good screening, the amplitude of the density variation is about 20% of the average density n_s (Fig. 2), so that $\Delta n_s/n_s \approx 0.14$. At filling factor $\nu=2$, the electron gas behaves more rigidly and does not follow the external modulation as well. As a consequence, the variance shows a dip, indicating the reduced screening ability of the 2D EG.

Figure 5 shows also a result for the higher temperature $T = 10$ K. In the ‘‘perfect screening’’ regime the screening becomes poorer, as is already expected from the linear approximation, since the thermodynamic DOS becomes smaller. At filling factor 2 screening becomes better (see also Fig. 4) since more states are available for the thermal redistribution of the electrons. An improvement of the screening properties of the 2D EG with increasing temperature for fully occupied Landau bands and very low temperature has recently also been observed experimentally.¹⁶

Figures 6 and 7 show results for a much stronger modulation of the external potential ($V_M = 60$ meV), leading to a stronger modulation of the electron density (Fig. 6). The screening properties depend now less drastically on the filling factor, but qualitatively the results for the Landau bands can be understood from the discussion given for the case $V_M = 25$ meV. To obtain a screened

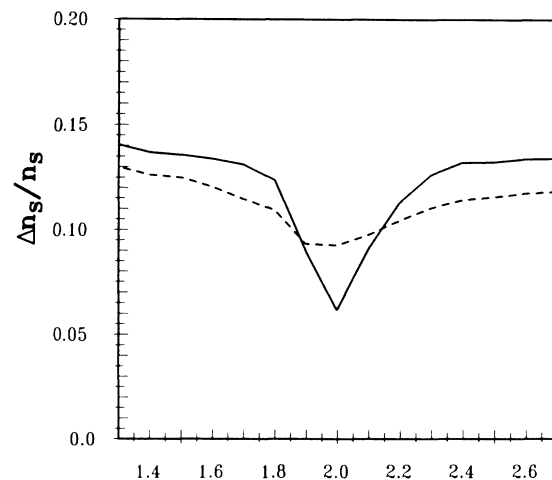


FIG. 5. Variance $\Delta n_s/n_s$ vs the filling factor for $V_M = 25$ meV at $T = 1$ K (solid line) and $T = 10$ K (dashed line).

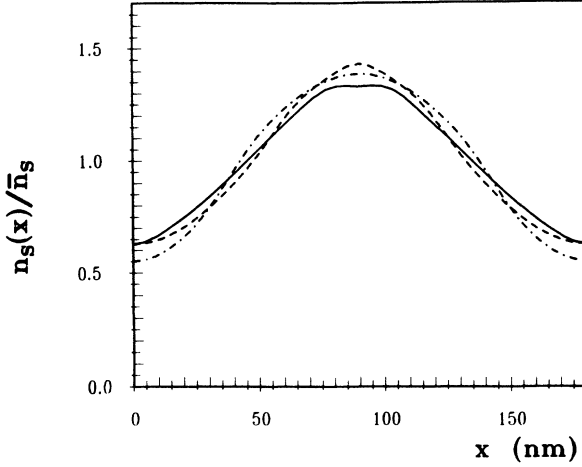


FIG. 6. Same as Fig. 2, but with $V_M = 60$ meV.

potential varying only by about $\hbar\omega_c$ for $\nu=2$, a substantial amount of electrons must be redistributed. This causes a slight overlap of the $n=0$ and $n=1$ bands (Fig. 7, $\nu=2$), and the density variation is not so strongly reduced.

The pinning of the energy spectrum to the Fermi level is for this large modulation clearly observed only in the lowest Landau level [Fig. 7(b)].

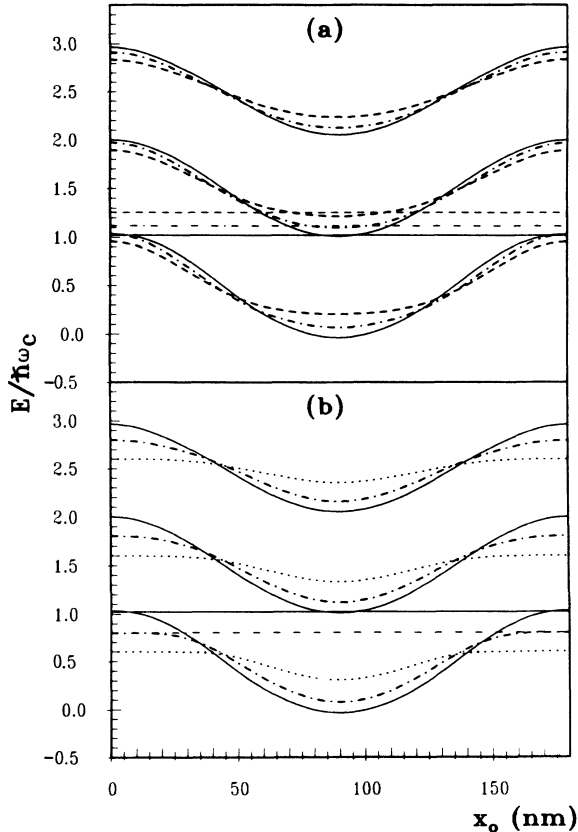


FIG. 7. Same as Fig. 3, but with $V_M = 60$ meV.

B. The two-dimensional model with boundaries

The diagonalization of the Hamiltonian was carried out within the subspace of wave functions of the three lowest Landau levels. The average electron density $n_s = n_b$ was kept constant at $n_s = 2.25 \times 10^{11} \text{ cm}^{-2}$ like in Sec. IV A and the magnetic field B was varied so that the filling factor for the spin-degenerate system never took a higher value than 2.6, i.e., the lowest LL filled but the second one is only partly occupied. In this case the inclusion of higher LL's in the diagonalization procedure did not change the results. This is, of course, only possible because we use the exact eigenfunctions of the noninteracting system in the bounded Teller geometry as basis functions.

Figure 8 demonstrates the effect of the boundary condition at $\pm \frac{1}{2}L_x = \pm 120$ nm. The broken lines refer to the noninteracting electron system with the electrostatic potential $V(x) \equiv 0$. The filling factor is $\nu=1.6$, so that the Fermi energy (not shown) is at $\frac{1}{2}\hbar\omega_c$, and edge states are not occupied. The solid lines refer to the corresponding Hartree result. As seen from Fig. 8(a), the electrons

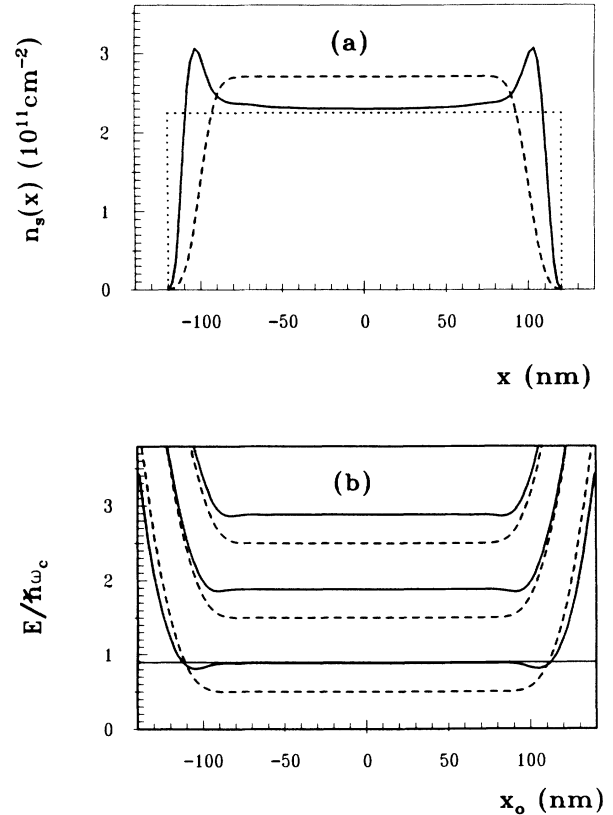


FIG. 8. (a) Electron density and (b) energy spectrum for $\nu=1.6$ and $T=1$ K from the strictly two-dimensional model with boundaries at $x = \pm 120$ nm and translational invariance in the y direction. The solid lines refer to the interacting system, the dashed lines to the corresponding noninteracting system. The dotted line in (a) indicates the density distribution of positive background charges, and the thin solid line in (b) gives the position of the Fermi level for the interacting system.

screen the positive background charge in the interior, the bulk, where the Landau bands are flat [Fig. 8(b)]. At the edges the electron density vanishes so that the net charge density there is positive. Since charge neutrality must hold, the system responds with peaks of $n_s(x)$ near $x = \pm 110$ nm, so that a dipole near each edge is formed. The superposition of the corresponding dipole potential with the free energy spectrum is seen in the calculated energy spectrum, which shows minima near the edge states with $x_0 = \pm 110$ nm. The occupation of these edge states leads to the peaks of $n_s(x)$. The width of the positively charged edge region is only of the order of the magnetic length l , i.e., of the extent of edge states (~ 20 nm). One obtains a similar result for the electron density if one considers the free, noninteracting electron system at a slightly higher filling factor, so that the edge states are occupied at an appreciable amount.

Figure 9 shows a situation, where the positive background is compressed to the layer $|x| < 74.4$ nm. Now the electron density leaks out from the background and at each of its edges a dipole is formed with negative charges at the outside. The corresponding potential keeps the electrons in the background region, so that they are practically not affected by the boundary conditions $\Phi(\pm 120 \text{ nm}) = 0$. The solid lines refer to the relatively good screening situation with a total filling factor $\nu = 1.1$,

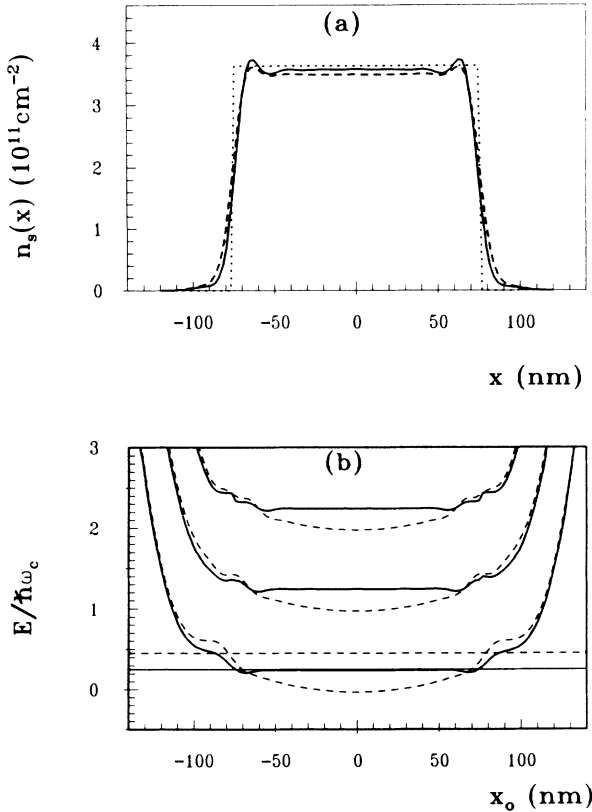


FIG. 9. Same as in Fig. 8, but for the interacting system at the filling factor $\nu = 1.1$ (solid lines) and $\nu = 1.3$ (dashed lines), respectively. Note that the same background charge is now compressed to the strip $|x| < 74.4$ nm.

which corresponds to an effective filling factor $\nu_{\text{eff}} = 1.8$ in the layer of the positive charges. We see a pronounced pinning of the $n = 0$ Landau band to the Fermi energy for x_0 values in the bulk region. The broken lines refer to the filling factor $\nu = 1.3$, i.e., $\nu_{\text{eff}} = 2.1$ in the background region. The screening is poorer, both in the bulk and the surface regions [Fig 9(a)]. The energy spectrum exhibits no flat regions and no pinning. We observed in all the considered situations that the energy spectrum develops a structure near the edges and adjusts in such a manner that the width of the edge region always is of the order of two or three times the magnetic length and depends only weakly on the filling factor.

In order to study the screening of a periodic perturbation, we modulated the positive background according to

$$n_b(x) = A(p, \alpha) n_s \left[1 + \alpha \cos \left(\frac{\pi x}{L_x} (2p + 1) \right) \right], \quad (4.2)$$

where

$$A(p, \alpha) = \left[1 + \frac{2\alpha}{\pi} \frac{(-1)^p}{2p + 1} \right]^{-1} \quad (4.3)$$

is a normalization factor ensuring $n_b = n_s$. L_x was chosen as $L_x = 240$ nm so that the width of the interior bulk region is comparable with the period chosen in Sec. IV A. The energy spectrum is shown in Fig. 10 for a 20% modulation of the background density, $\alpha = 0.2$, three different periods, $p = 1, 2$, and 8, and, in all cases, for the filling factors $\nu = 1.6, 2.0$, and 2.4. The screening behavior seen in Fig. 10(a) is similar to that found in Fig. 3. For $\nu = 1.6$ (solid curves) screening in the bulk region is very good, the Landau bands in the bulk region are very small, and the (relative) maxima of the $n = 0$ band are pinned to the Fermi level. For $\nu = 2.4$ (dash-dotted curves), the screening is again very good, the width of the Landau bands in the bulk region is small, and the minimum of the $n = 1$ band is in a wide region pinned to the Fermi level. For $\nu = 2$ (dotted lines), the screening properties are much poorer. Broad levels with considerable oscillations are observed. The Fermi level touches the minimum of the $n = 1$ band but not the maximum of the $n = 0$ band, as might be expected from the corresponding calculation without edges (cf., Fig. 3).

The explanation is, however, simple. The modulation is chosen such that the density of positive background charges is lowered in the edge regions. Thus, the potential created by the background enhances the effect of the boundary conditions to push the electrons away from the edges into the bulk region. As a consequence, the effective filling factor in the bulk region is somewhat larger than the overall filling factor ν . Therefore, the poorest screening in the bulk is expected at a somewhat smaller value of ν . This is indeed what we see in Fig. 11(a), where we have plotted the variance $\Delta n_s / n_s$ defined in Eq. (4.1). The electron gas behaves most rigidly, i.e., the screening is poorest, for a ν value close to 1.9.

Figure 10(b) shows the energy spectrum for a smaller period of the modulated background density, which means also a smaller amplitude of the modulation poten-

tial [cf. Eq. (2.5)]. Whereas there is still relatively good screening in the bulk region for $\nu=1.6$, the screening is poorer for $\nu=2.4$. For $\nu=2$, we observe poor screening and the Fermi level is kept in the gap between the minima of the $n=1$ band and the maxima of the $n=0$ band by the edge states only. The electron densities for $\nu=1.6$ and $\nu=2.0$ are compared with the modulated background density in Fig. 12.

The modulation period chosen in Fig. 10(c) is not much larger than $2l$, i.e., the extent of the wave function $\Phi_{0,x_0}(x)$. The screening is poor for all filling factors, although the amplitude of the modulating potential is small. The oscillations in the $n=0$ Landau band and in the $n=1$ Landau band show opposite phases. This indicates that the corresponding wave functions average over potential regions with different behavior, e.g., minima instead of maxima. These results are easily understood within a simple approximation which is valid in the interior bulk region, where the eigenfunctions of the unmo-

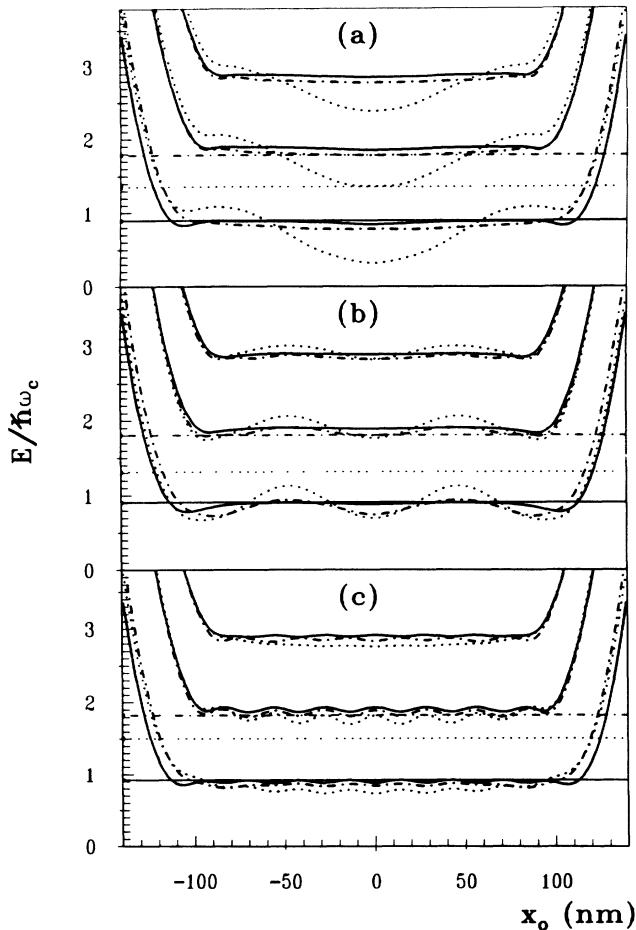


FIG. 10. Energy spectrum (thick lines) and Fermi energy (thin horizontal lines) for the strip model ($|x| < 120$ nm) with 20% modulation of the background density according to Eq. (4.2). The modulation parameters are $\alpha=0.2$ and (a) $p=1$, (b) $p=2$, and (c) $p=8$ for the periods. Results are shown for the filling factors $\nu=1.6$ (solid lines), 2.0 (dotted lines), and 2.4 (dash-dotted lines).

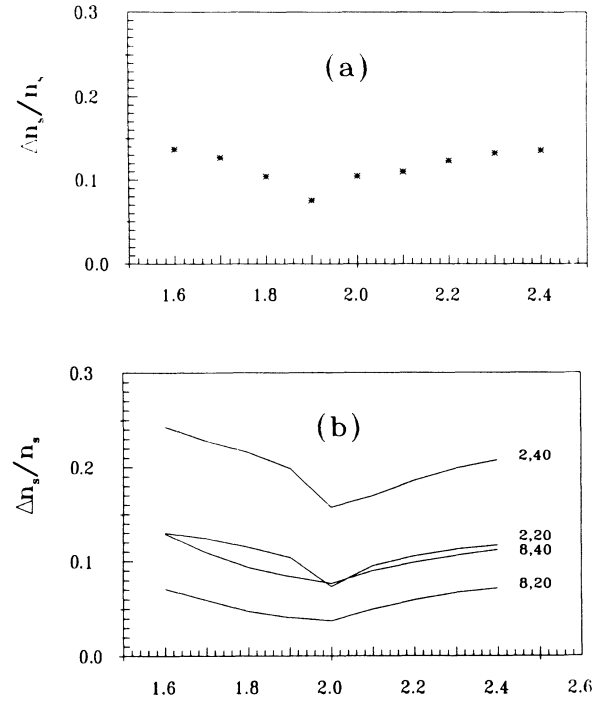


FIG. 11. Variance of the electron density vs filling factor for the strip model with different modulations of the background density: (a) $p=1$, $\alpha=0.2$ as in Fig. 10(a); (b) $p=2$ and $p=8$ for 20% and for 40% modulation. The pairs of numbers labeling the curves indicate p and 100α .

ulated system are usual Landau wave functions. Owing to the small amplitude of the effective modulation potential, $l |dV/dx| \ll \hbar\omega_c$ holds and level mixing is again small. Assuming a harmonic variation of the screened potential with period $a=2\pi/k$, $V(x)=V_0\cos(kx)$, first-order perturbation theory yields³⁰

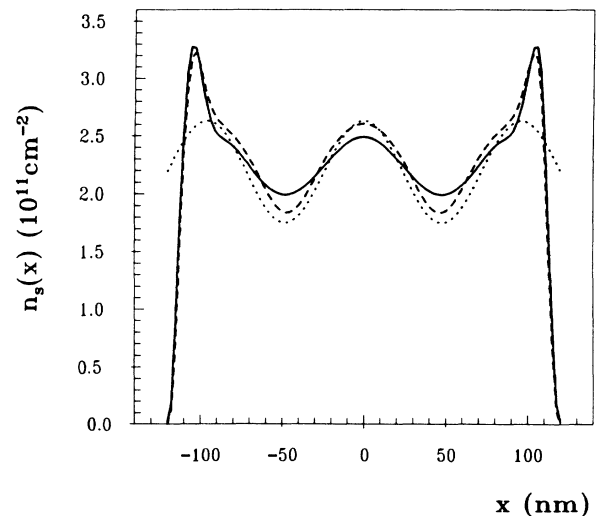


FIG. 12. Electron density for the strip model with a modulated background density ($p=2$, $\alpha=0.2$), indicated by the dotted line, for filling factors $\nu=2.0$ (solid curve) and $\nu=1.6$ (dashed curve) at $T=1$ K.

$$E_{n,x_0} = \hbar\omega_c(n + \frac{1}{2}) + V(x_0)\exp(-\frac{1}{4}k^2l^2)L_n(\frac{1}{2}k^2l^2), \quad (4.4)$$

where L_n is a Laguerre polynomial. For the dotted curves of Fig. 10(c) ($\nu=2.0$), $\frac{1}{2}k^2l^2 \approx 3.5$ and $L_0=1$, $L_1=-2.5$, and $L_2 \approx 0.1$. For the solid lines ($\nu=1.6$) the L_n assume the values 1, -1.8 , and -0.6 , and for the dash-dotted lines ($\nu=2.4$) the values 1, -3.2 , and 1.2 . This nicely explains the relative phases of the oscillations. For larger periods, $\frac{1}{2}k^2l^2 \ll 1$, the factor of $V(x_0)$ in Eq. (4.4) approaches unity, and the low-lying Landau bands become nearly parallel, as seen in Figs. 3 and 7.

Figure 11(b) shows the variance $\Delta n_s/n_s$ corresponding to the modulations considered in Figs. 10(b) and 10(c), ($\alpha=0.2$, $p=2$ and 8), together with similar results obtained for modulations with larger amplitude ($\alpha=0.40$, $p=2$ and 8). As in Fig. 5, we observe the poorest screening, i.e., the most rigid electron density, for $\nu=2$. For the large period modulations ($p=2$, $\alpha=0.2$ and 0.4), the variance of the electron density at $\nu=1.6$ is only about 5–10% smaller than the variance of the background charge density. For the small period modulation ($p=8$, $\alpha=0.2$ and 0.4), on the other hand, the variance of the electron density for $\nu=1.6$ is about a factor of 2 smaller than the variance of the background charge density. This again indicates that the screening of the small-period fluctuations is considerably poorer.

V. SUMMARY

Within the Hartree approximation, we have calculated ground-state properties of a two-dimensional electron gas in a quantizing magnetic field and a modulating external potential which lifts the degeneracy of the Landau levels. Translation invariance in the y direction was assumed, so that the center coordinate $x_0 = -l^2k_y$ is a good quantum number for the discussion of the energy dispersion $E_n(x_0)$ where n labels the Landau bands.

For partly occupied Landau levels, with the Fermi energy well within a broadened level, we find nearly perfect screening of the external potential, in agreement with the linear screening approximation sketched in Sec. II. In this situation the width of the Landau bands is very small.

If a Landau level is nearly full or nearly empty, screening breaks down in some parts of the sample whereas in others perfect screening pertains leading to a pinning of the energy spectrum to the Fermi energy. Such highly nonlinear screening properties have been predicted by Luryi² on the basis of qualitative arguments. He anticipated that the density of states should have a sharp peak at the Fermi level, which repeats in the other LL's. Our results confirm this only to a certain extent, since the calculated Landau bands as a function of the center coordinate are not completely parallel, and since the pinning effect is less pronounced in higher Landau levels. More-

over, all minima and maxima of the E_n -versus- x_0 curves lead to sharp peaks of the DOS in our calculation, since we have not included an intrinsic collision broadening. Nevertheless, we find that the Landau bands become considerably broader if the levels are nearly full or nearly empty and that, owing to the pinning effect, the DOS at the Fermi energy is always relatively high.

The maximum width of the Landau bands is obtained for just completely filled LL's. For the large amplitude modulation potentials considered in the strictly periodic model, we found that the maximum width of the Landau bands, and also the total variation of the screened potential is just the cyclotron energy $\hbar\omega_c$, independent of the strength of the external potential modulation. This result, caused by the highly nonlinear screening properties of the system, will, of course, hold only if the total variation of the external potential is neither too small, e.g., less than $\hbar\omega_c$, nor too large, so that screening breaks down totally.

Interpreting our results in terms of a single-particle density of states, we obtain a nice justification of the inhomogeneity model,^{21–23} which dealt with screening on the basis of phenomenological model assumptions. We see that the linewidth of the Landau levels depends on the collective state of the 2D EG and oscillates with the filling factor of the LL's. Since we have neglected collision broadening effects, we got a very small width for close to half-filled LL's, but a large width of the order of $\hbar\omega_c$ for complete filling. Also the results for the variance of the electron density as a function of the filling factor (Figs. 5 and 11) confirm the behavior anticipated by a phenomenological calculation within the " n_{s0} -Gaussian" statistical model.²³

Finally we want to comment on the relevance of our results for the understanding of the integer quantum Hall effect, which is usually discussed within a single-particle picture. As mentioned in the Introduction, large fluctuations of the external donor potential on a mezzoscopic scale must be expected,²⁵ at least for $\text{Al}_x\text{Ga}_{1-x}\text{As}$ heterostructures. Therefore, the screening effects discussed in the present work must be important in the quantum Hall regime. In Si MOSFET's the situation is similar, as we know from the luminescence measurements of the density of states.^{15,16} As a consequence, in the plateau regime of the integer quantum Hall effect, i.e., for nearly full or nearly empty LL's, we have to expect quasiclassical localization of the electrons in the large, long-range potential fluctuations, which will be screened out completely for half-filled LL's. Thus, the breakdown of metallic screening may be the relevant localization mechanism responsible for the integer quantum Hall effect.

ACKNOWLEDGMENT

We gratefully acknowledge support of the Bundesministerium für Forschung und Technologie, West Germany (under Grant No. NT-2718-C).

- ¹For recent work in this field, see *High Magnetic Fields in Semiconductor Physics*, Vol. 71 of *Springer Series in Solid-state Sciences*, edited by G. Landwehr (Springer, Berlin, 1987).
- ²S. Luryi, in *High Magnetic Fields in Semiconductor Physics*, Ref. 1, p. 16.
- ³D. Weiss, K. v. Klitzing, and V. Mosser, in *Two-Dimensional Systems: Physics and New Devices*, Vol. 67 of *Springer Series in Solid-State Sciences*, edited by G. Bauer, F. Kuchar, and H. Heinrich (Springer, Berlin, 1986), p. 204.
- ⁴T. P. Smith, B. B. Goldberg, P. J. Stiles, and M. Heiblum, *Phys. Rev. B* **32**, 2696 (1985).
- ⁵V. Mosser, D. Weiss, K. v. Klitzing, K. Ploog, and G. Weimann, *Solid State Commun.* **58**, 5 (1985).
- ⁶D. Weiss and K. v. Klitzing, in *High Magnetic Fields in Semiconductor Physics*, Ref. 1, p. 57.
- ⁷B. Tausendfreund and K. v. Klitzing, *Surf. Sci.* **142**, 220 (1984).
- ⁸E. Stahl, D. Weiss, G. Weimann, K. v. Klitzing, and K. Ploog, *J. Phys. C* **18**, L783 (1985).
- ⁹M. G. Gavrilo and I. V. Kukushkin, *Pis'ma Zh. Eksp. Teor. Fiz.* **43**, 79 (1986) [*JETP Lett.* **43**, 103 (1986)].
- ¹⁰R. T. Zeller, F. F. Fang, B. B. Goldberg, S. L. Wright, and P. J. Stiles, *Phys. Rev. B* **33**, 1529 (1986).
- ¹¹D. Weiss, V. Mosser, V. Gudmundsson, R. R. Gerhardtts, and K. v. Klitzing, *Solid State Commun.* **62**, 89 (1987).
- ¹²E. Gornik, R. Lassnig, G. Strasser, H. L. Störmer, A. C. Gossard, and W. Wiegmann, *Phys. Rev. Lett.* **54**, 1820 (1985).
- ¹³J. P. Eisenstein, H. L. Störmer, V. Narayanamurti, A. Y. Cho, A. C. Gossard, and C. W. Tu, *Phys. Rev. Lett.* **55**, 875 (1985).
- ¹⁴D. Heitmann, M. Ziesmann, and L. L. Chang, *Phys. Rev. B* **34**, 7463 (1986).
- ¹⁵I. V. Kukushkin and V. B. Timofeev, *Pis'ma Zh. Eksp. Teor. Fiz.* **43**, 387 (1986) [*JETP Lett.* **43**, 499 (1986)]; see also Ref. 1, p. 282.
- ¹⁶I. V. Kukushkin and V. B. Timofeev, *Zh. Eksp. Teor. Fiz.* **93**, 1122 (1987) [*Sov. Phys. - JETP* (to be published)].
- ¹⁷R. Lassnig and E. Gornik, *Solid State Commun.* **47**, 959 (1983).
- ¹⁸T. Ando and Y. Murayama, *J. Phys. Soc. Jpn.* **54**, 1519 (1985).
- ¹⁹W. Cai and T. S. Ting, *Phys. Rev. B* **33**, 3967 (1986).
- ²⁰Y. Murayama and T. Ando, *Phys. Rev. B* **35**, 2252 (1987).
- ²¹R. R. Gerhardtts and V. Gudmundsson, *Phys. Rev. B* **34**, 2999 (1987).
- ²²V. Gudmundsson and R. R. Gerhardtts, in *High Magnetic Fields in Semiconductor Physics*, Ref. 1, p. 6.
- ²³V. Gudmundsson and R. R. Gerhardtts, *Phys. Rev. B* **35**, 8005 (1987).
- ²⁴R. R. Gerhardtts, *Z. Phys. B* **21**, 275 (1975); **21**, 285 (1975); *Surf. Sci.* **58**, 234 (1976).
- ²⁵B. I. Shklovskii and A. L. Éfros, *Pis'ma Zh. Eksp. Teor. Fiz.* **44**, 520 (1986) [*JETP Lett.* **44**, 669 (1987)].
- ²⁶W. Hansen, M. Horst, J. P. Kotthaus, U. Merkt, Ch. Sikorski, and K. Ploog, *Phys. Rev. Lett.* **58**, 2586 (1987).
- ²⁷J. Labbé, *Phys. Rev. B* **35**, 1373 (1987).
- ²⁸U. Wulf, *Phys. Rev. B* **35**, 9754 (1987).
- ²⁹V. Gudmundsson, R. R. Gerhardtts, R. Johnston, and L. Schweitzer *Z. Phys. B* **70**, 453 (1988).
- ³⁰A. V. Chaplik, *Solid State Commun.* **53**, 539 (1985).